ISSN 2472-1972

Phosphoinositide 3-Kinase Is Integral for the Acute Activity of Leptin and Insulin in Male Arcuate NPY/AgRP Neurons

Yiru Huang,[1,2]* Zhenyan He,[1,2]* Yong Gao,[2,3]* Linh Lieu,[2]* Ting Yao,[2] Jia Sun,[2] Tiemin Liu,[2] Chris Javadi,[2] Maria Box,[2] Sadia Afrin,[2] Hongbo Guo,[1] and Kevin W. Williams[2]

[1]The National Key Clinical Specialty, The Engineering Technology Research Center of Education Ministry of China, Guangdong Provincial Key Laboratory on Brain Function Repair and Regeneration, Department of Neurosurgery, Zhujiang Hospital, Southern Medical University, Guangzhou 510282, China; [2]Division of Hypothalamic Research, The University of Texas Southwestern Medical Center, Dallas, Texas 75390; and [3]National Laboratory of Medical Molecular Biology, Institute of Basic Medical Sciences, Chinese Academy of Medical Sciences and Peking Union Medical College, Beijing 100005, China

*These authors are co-first authors.

Neuropeptide Y (NPY)/Agouti-related protein (AgRP) neurons in the arcuate nucleus of the hypothalamus are part of a neuroendocrine feedback loop that regulates feeding behavior and glucose homeostasis. NPY/AgRP neurons sense peripheral signals (including the hormones leptin, insulin, and ghrelin) and integrate those signals with inputs from other brain regions. These inputs modify both long-term changes in gene transcription and acute changes in the electrical activity of these neurons, leading to a coordinated response to maintain energy and glucose homeostasis. However, the mechanisms by which the hormones insulin and leptin acutely modify the electrical activity of these neurons remain unclear. In this study, we show that loss of the phosphoinositide 3-kinase catalytic subunits p110α and p110β in AgRP neurons abrogates the leptin- and insulin-induced inhibition of AgRP neurons. Moreover, continual disruption of p110α and p110β in AgRP neurons results in increased weight gain. The increased adiposity was concomitant with a hypometabolic phenotype: decreased energy expenditure independent of changes in food intake. Deficiency of p110α and p110β in AgRP neurons also impaired glucose homeostasis and insulin sensitivity. In summary, these data highlight the requirement of both p110α and p110β in AgRP neurons for the proper regulation of energy balance and glucose homeostasis.

Freeform/Key Words: diabetes, energy balance, glucose homeostasis, melanocortin, obesity, patch-clamp

The increasing incidence of obesity and diabetes implores a need to better understand neurobiological and physiological mechanisms regulating energy balance and glucose metabolism. Acute activation of neuropeptide Y/Agouti-related peptide (NPY/AgRP)–expressing neurons restricted to the arcuate (ARC) nucleus of hypothalamus evokes voracious feeding while concomitantly impairing energy expenditure and glucose homeostasis [1–4]. Conversely, inhibition of NPY/AgRP neuronal activity rapidly suppresses feeding

Abbreviations: ACSF, artificial cerebrospinal fluid; AgRP, Agouti-related protein; APT, AgRP-cre::p110$\alpha^{fl/fl}$::p110$\beta^{fl/fl}$::tdTomato; ARC, arcuate; CNQX, 6-cyano-7-nitroquinoxaline-2,3-dione; hrGFP, humanized Renilla green fluorescent protein; InsR, insulin receptor; K_{ATP}, ATP-sensitive K^+; LepR, leptin receptor; NLT, NPY-hrGFP::LepR-cre::tdTomato; NPY, neuropeptide Y; PI3K, phosphoinositide 3-kinase; POMC, pro-opiomelanocortin; TTX, tetrodotoxin.

Received 27 February 2018
Accepted 23 April 2018
First Published Online 26 April 2018

behavior [3, 5]. Several circulating factors including leptin and insulin have been suggested to suppress the acute activity of NPY/AgRP neurons. The inhibitory effects of leptin and insulin in NPY/AgRP neurons have been directly associated with that of phosphoinositide 3-kinase (PI3K) [6–11]. Thus, a cellular mechanism of leptin and insulin action within the brain to regulate energy balance and glucose homeostasis has been proposed to require at least in part PI3K activity in NPY/AgRP neurons [8, 12, 13].

PI3Ks act in the hypothalamus as dimers of a catalytic subunit (p110α or p110β) and a p85 regulatory subunit [14]. Interestingly, p110β appears to have a dominant role in NPY/AgRP neurons, as mice deficient for p110β in AgRP neurons are lean and display hypoleptinemia. However, selective deletion of either p110α or p110β catalytic subunits alone in NPY/AgRP neurons fails to alter fasting glucose levels, glucose tolerance, or fasting insulin levels [8]. Moreover, deficiency of either p110α or p110β in NPY/AgRP neurons alone fails to diminish the acute cognate effects of leptin and insulin in NPY/AgRP neurons [8]. Importantly, the presence of one p110 isoform may be sufficient to compensate for the loss of the other, providing evidence for a functional redundancy of p110 isoforms in various tissues [15, 16]. As a result, deletion of both p110α and p110β isoforms may provide a more direct test of the PI3K dependence of leptin and insulin responses in NPY/AgRP neurons as well as PI3K activity on metabolism. In the current study, the hypothesis that both p110α and p110β are required for the acute inhibition of NPY/AgRP neurons by leptin and insulin was tested using whole-cell recordings in hypothalamic slices from mice. Acute effects of leptin and insulin were assessed on intrinsic membrane properties of NPY/AgRP neurons, including subsets of leptin receptor (LepR)–positive and –negative NPY neurons. The requirement of p110α and p110β in AgRP neurons to regulate energy balance and glucose homeostasis was also assessed. Together, these data provide a possible cellular mechanism in which PI3K regulates energy balance and glucose homeostasis via NPY/AgRP neuronal activity.

1. Materials and Methods

A. Animals

Male mice were used for all experiments. All mice were housed under standard laboratory conditions (12 hours on/off; lights on at 7:00 AM) and temperature-controlled environment with food and water available *ad libitum*. All experiments were performed in accordance with the guidelines established by the National Institutes of Health Guide for the Care and Use of Laboratory Animals and approved by The University of Texas Institutional Animal Care and Use Committee. Mice were provided a Harlan Teklad 2016 chow diet or high-fat/high-sucrose (D12331; Research Diets) diet and water *ad libitum* unless otherwise noted. Mice that incurred a 10% body weight loss during the acclimation period for metabolic cage studies (described later) were not used. Body weight was measured weekly and body composition was measured by using nuclear magnetic resonance (Bruker minispec; Bruker Corporation).

To identify NPY neurons with or without LepRs, we generated NPY-hrGFP::LepR-cre::tdTomato (NLT) mice as previously described [17], anatomically restricted to the ARC nucleus of the hypothalamus. Briefly, LepR reporter mice were made by mating LepR-cre mice [18] with the tdTomato reporter mouse (#007908; The Jackson Laboratory). LepR-cre::tdTomato reporter mice were subsequently mated with NPY-humanized Renilla green fluorescent protein (hrGFP) mice [19] to produce NPY-hrGFP::LepR-cre::tdTomato (NLT) mice. For inactivation of both p110α and p110β on AgRP neurons, we crossed mice carrying a conditional mutation in the PI3K catalytic subunits Pik3ca (p110α) and Pik3cb (p110β) [20, 21] with transgenic mice expressing cre driven by the AgRP promoter [22], followed by interbreeding with tdTomato mice [AgRP-cre::p110$\alpha^{fl/fl}$::p110$\beta^{fl/fl}$::tdTomato (APT)]. A separate cohort of mice were generated that were deficient for both LepR and insulin receptor (InsR) in AgRP neurons by breeding AgRP-cre mice with mice containing a conditional mutation in the LepR and InsR [23, 24]. These mice were then crossed with tdTomato mice (AgRP-cre::LepR$^{fl/fl}$::InsR $^{fl/fl}$::tdTomato).

B. Metabolic Chambers

Experiments were performed in a temperature-controlled room containing 36 TSE Systems metabolic cages maintained by The University of Texas Southwestern Animal Resources personnel. One week prior to the study, mice were singly housed to acclimate to new housing. Three days prior to the study, mice were transported to the room containing the metabolic cages to acclimate to a new environment. A high-fat/high-sucrose diet, if applicable, was also introduced at the beginning of this acclimation period. After 3 days' acclimation, cages were connected to the TSE Systems for a total of 5 days. Days 2 to 4 were used for data analyses.

C. Glucose Tolerance Tests

After an overnight fast, 10- to 14-week-old male mice received IP injections of 1.5 g/kg D-glucose. Blood glucose was measured from tail blood using a glucometer at serial time points as indicated in the figures.

D. Insulin Tolerance Tests

After a 4-hour fast to empty the stomach, 10- to 14-week-old male mice received IP injections of insulin (1.2 units/kg). Blood glucose was measured from tail blood as described previously.

E. Pyruvate Tolerance Tests

After a 6-hour fast to empty the stomach, 10- to 14-week-old male mice received IP injections of 2 mg/kg pyruvate. Blood glucose was measured from tail blood as described previously.

F. Analysis of Gene Expression by Quantitative PCR

Total RNA was extracted from tissues with TRIzol reagent (Invitrogen) according to the manufacturer's instructions. Total RNA (1 mg) was converted into first-strand cDNA with oligo(dT) primers as described by the manufacturer (Clontech). PCR was performed in an Mx3000P Q-PCR system (Stratagene) with specific primers and SYBR Green PCR Master Mix (Stratagene). The relative abundance of mRNAs was standardized with 18S mRNA as the invariant control.

G. Electrophysiology Studies

Brain slices were prepared from young adult male mice (6 to 12 weeks old) as previously described [25, 26]. Briefly, male mice were deeply anesthetized with an IP injection of 7% chloral hydrate and transcardially perfused with a modified ice-cold artificial cerebrospinal fluid (ACSF; described later). The mice were then decapitated, and the entire brain was removed and immediately submerged in ice-cold, carbogen-saturated (95% O_2 and 5% CO_2) ACSF (126 mM NaCl, 2.8 mM KCl, 1.2 mM $MgCl_2$, 2.5 mM $CaCl_2$, 1.25 mM NaH_2PO_4, 26 mM $NaHCO_3$, and 5 mM glucose). Coronal sections (250 μm) were cut with a VT1000S Vibratome (Leica Microsystems) and then incubated in oxygenated ACSF at room temperature for at least 1 hour before recording. The slices were bathed in oxygenated ACSF (32°C to 34°C) at a flow rate of ~2 mL/min. All electrophysiology recordings were performed at room temperature.

The pipette solution for whole-cell recording was modified to include an intracellular dye (Alexa Fluor 350 hydrazide dye) for whole-cell recording: 120 mM K-gluconate, 10 mM KCl, 10 mM HEPES, 5 mM EGTA, 1 mM $CaCl_2$, 1 mM $MgCl_2$, 2 mM ATP, and 0.03 mM Alexa Fluor 350 hydrazide dye (pH 7.3). Epifluorescence was briefly used to target fluorescent cells, at which time the light source was switched to infrared differential interference contrast imaging to obtain the whole-cell recording [Axioskop FS2 Plus equipped with a fixed stage (Zeiss) and a QuantEM:512SC electron-multiplying charge-coupled device camera (Photometrics)]. Electrophysiological signals were recorded using an Axonpatch 700B amplifier (Molecular Devices), low-pass filtered at 2 to 5 kHz, and analyzed offline on a personal

computer with pCLAMP programs (Molecular Devices). Membrane potential and firing rate were measured by whole-cell current clamp recordings from NPY/AgRP neurons in brain slices. Recording electrodes had resistances of 2.5 to 5 MΩ when filled with the K-gluconate internal solution. Input resistance was assessed by measuring voltage deflection at the end of the response to hyperpolarizing rectangular current pulse steps (500 ms of −10 to −50 pA).

Solutions containing drugs were typically perfused for 5 minutes. A drug effect was required to be associated temporally with peptide application, and the response had to be stable within a few minutes. A neuron was considered depolarized or hyperpolarized if a change in membrane potential was at least 2 mV in amplitude.

H. Drugs

Leptin (100 nM; provided by A. F. Parlow through the National Hormone and Peptide Program), Humulin (50 nM; Eli Lilly and Company), tolbutamide (200 μM; Sigma-Aldrich), tetrodotoxin (TTX; 2 μM; Tocris Bioscience), LY294002 (10 μM; Calbiochem), wortmannin (100 nM; Tocris Bioscience), 6-cyano-7-nitroquinoxaline-2,3-dione (CNQX; 10 μM; Sigma-Aldrich), AP5 (50 μM; Sigma-Aldrich), and picrotoxin (50 μM; Sigma-Aldrich) were added to the ACSF for specific experiments. All solutions were made according to the manufacturer's specifications. Stock solutions of LY294002, wortmannin, CNQX, and picrotoxin were made by dissolution in dimethyl sulfoxide (Sigma-Aldrich). The concentration of dimethyl sulfoxide in the external solution was <0.1%. Stock solutions of leptin were made by dissolution in Dulbecco's PBS (Gibco). Stock solutions of TTX and AP5 were made by dissolution in deionized water.

I. Cell Counting

Cell counts of LepR- and NPY-expressing ARC neurons were performed as previously described [27–29]. Briefly, the male NLT mice (n = 6; male) were anesthetized, transcardially perfused with the 0.95% saline for 1 minute, and then shift to the 10% neural buffered formalin for 6 to 8 minutes. The mice were then decapitated, and the entire brain was removed, fixed by 10% neural buffered formalin for 4 hours at room temperature, and cryopreserved in 30% sucrose at 4°C overnight. Brains were then sectioned into 25-μm coronal sections and separated equally into five series. The slices were stored in cryoprotectant at −20°C until use. Counts of GFP- and tdTomato-labeled cells were made using ImageJ software (National Institutes of Health) by an observer who was blinded to the condition or genotype of the mice with the aid of a Zeiss microscope. Sections that come from two series were viewed at 10 magnifications, and the number of reporters labeled cells was quantified in the retrochiasmatic area and ARC. Counts from the retrochiasmatic area and ARC were obtained from maximal rostrocaudal area of each brain (n = 6), corresponding to the planes from 0.94 mm to 2.80 mm posterior to bregma in the Paxinos and Franklin atlas [30].

J. Analysis and Statistics

Results are reported as the mean ± SEM unless indicated otherwise, in which n represents the number of cells studied. Significance was set at $P < 0.05$ for all statistical measures.

2. Results

A. AgRP-Specific Disruption of Both p110α and p110β Exacerbates Body Weight Gain

To determine the requirement of both p110α and p110β in AgRP neurons for the maintenance of energy homeostasis, we monitored metabolic parameters in mice with p110α and p110β double deficiency (AgRP-cre::p110$\alpha^{fl/fl}$::p110$\beta^{fl/fl}$) on a chow diet. Deletion of p110α and p110β in ARC AgRP neurons was validated in study subjects (Supplemental Fig. 1). Mice deficient

for both p110α and p110β in AgRP neurons displayed an age-dependent increase in body weight concurrent with increased fat and lean mass (*$P < 0.05$; Fig. 1A and 1B). When compared with their control littermates, mice deficient for p110α and p110β in AgRP neurons displayed decreased energy expenditure independent of changes in food intake or activity levels (Fig. 1C–1F), supporting a requirement of both p110α and p110β AgRP neurons for the proper regulation of energy balance. Similar results were obtained when mice were placed on a high-fat diet (Supplemental Fig. 2A).

B. Inactivation of Both p110α and p110β in AgRP Neurons Impairs Glucose and Insulin Sensitivity

In addition to impairments of energy homeostasis, simultaneous p110α and p110β deficiency in AgRP neurons induced systemic glucose intolerance and insulin resistance independent of diet (Fig. 2A and 2B; Supplemental Fig. 2B and 2C). Moreover, when pyruvate was provided as a fuel source, AgRP-cre::p110$\alpha^{fl/fl}$::p110$\beta^{fl/fl}$ mice produced higher levels of glucose compared with littermate controls (Fig. 2C). We next considered the effects on glucose production in the liver by using quantitative real-time quantitative reverse transcription polymerase chain reaction to examine genes within the liver that play a role in gluconeogenesis. AgRP-specific deletion of p110α and p110β showed increased mRNA levels of *Foxo1, G6pc, HNF4*α, *pcx,* and *pepck* in the liver (Fig. 2D), supporting a role for AgRP-specific deletion of p110α and p110β to enhance hepatic glucose production.

C. The Leptin-Induced Hyperpolarization of LepR-Positive NPY Neurons Requires Both p110α and p110β

The distribution of ARC NPY/AgRP neurons that express or do not express LepRs was mapped from NLT mice. We found 64.1% of NPY-hrGFP neurons restricted to the ARC nucleus were positive for LepRs, whereas 52.4% of LepR-positive ARC neurons also expressed NPY-hrGFP (Supplemental Table 1 and Supplemental Fig. 3). Both LepR-positive and -negative ARC NPY/AgRP neurons were targeted for electrophysiological recordings.

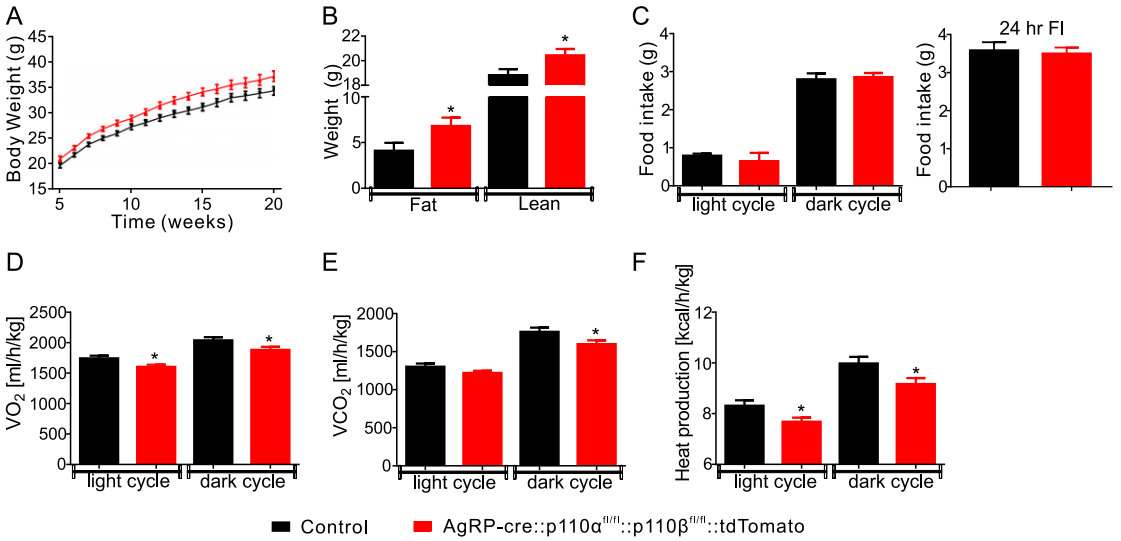

Figure 1. AgRP-specific disruption of both p110α and p110β exacerbates body weight gain and suppresses energy expenditure. (A) Body weight curve of male AgRP-cre::p110$\alpha^{fl/fl}$::p110$\beta^{fl/fl}$ mice on a chow diet. (B) Body composition of male AgRP-cre::p110$\alpha^{fl/fl}$::p110$\beta^{fl/fl}$ mice on a chow diet. (C) Double deletion of p110α and p110β in AgRP neurons does not affect food intake (FI). AgRP-specific disruption for both p110α and p110β suppresses (D) oxygen uptake (VO_2), (E) carbon dioxide production (VCO_2), and (F) heat production (10 weeks). Error bars indicate SEM. *$P < 0.05$.

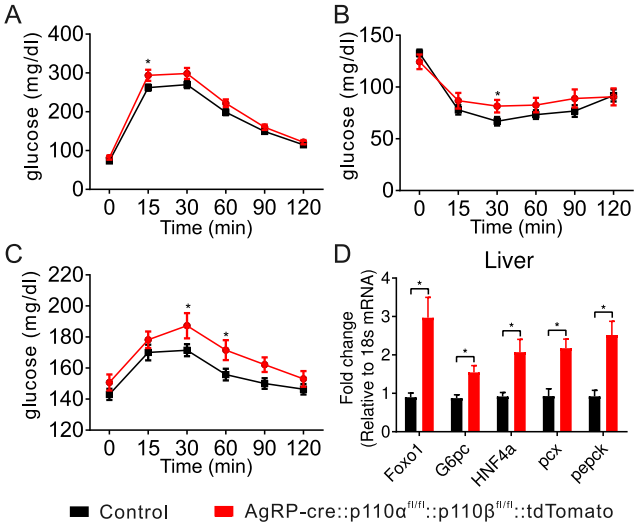

Figure 2. Inactivation of both p110α and p110β in AgRP neurons impairs glycemia and insulin sensitivity. Inactivation of both p110α and p110β in AgRP neurons impairs (A) glucose tolerance and (B) insulin sensitivity and (C) increases hepatic glucose production. (D) AgRP-specific deletion of p110α and p110β increases mRNA levels of *Foxo1, G6pc, HNF4*α*, pcx,* and *pepck*. Error bars indicate SEM. *$P < 0.05$.

Real-time visualization under fluorescence microscopy and Alexa Fluor 350 hydrazide dye was used to dialyze neurons recorded (Fig. 3A–3E). Consistent with the previous reports [7, 31], a majority of LepR-positive NPY-hrGFP neurons were hyperpolarized by local administration of leptin [100 nM; 79%; change in resting membrane potential (RMP): −9.9 ± 1.2 mV; resting membrane potential: −44.7 ± 1.1 mV; n = 30; Fig. 3F]. The remaining neurons failed to respond to leptin (change in RMP: −0.5 ± 0.4 mV; resting membrane potential: −43.2 ± 1.9 mV; n = 8; data not shown). The hyperpolarization induced by leptin (100 nm) was also observed in the presence of TTX (2 μm; 72%, change in RMP: −10.1 ± 2.1 mV; resting membrane potential: −42.7 ± 1.9 mV; n = 11; data not shown), indicative of a direct membrane hyperpolarization independent of action potential–mediated synaptic transmission. Additionally, application of leptin on LepR-positive NPY-hrGFP neurons reduced the firing frequency concomitant with a decrease in input resistance (25%; 1600 ± 53 MΩ for control, 1200 ± 101 MΩ for leptin; reversal potential of −90 ± 2.3 mV; n = 8; Fig. 3G and 3H). Subsequent application of tolbutamide (200 μM) following leptin administration completely reversed the hyperpolarization of LepR-positive NPY-hrGFP neurons induced by leptin (n = 12) (Fig. 3I). All LepR-negative NPY-hrGFP neurons tested were unresponsive to leptin (change in RMP: −0.6 ± 1.4 mV; n = 13; Fig. 3J). Moreover, AgRP neurons deficient for LepRs (AgRP-cre::LepR-flox::tdTomato) failed to respond to leptin (change in RMP: −0.3 ± 0.3 mV; n = 10; Supplemental Fig. 4). Collectively, these data support a leptin-induced hyperpolarization of LepR-positive NPY-hrGFP neurons that is dependent upon activation of an ATP-sensitive K^+ (K_{ATP}) channel.

To determine the involvement of PI3K in mediating leptin-induced hyperpolarization of NPY neurons, we introduced PI3K antagonists wortmannin and LY294002 to brain slices containing the ARC followed by application of leptin. Pretreatment with wortmannin (100 nM; 10 minutes) blocked the leptin-induced hyperpolarization of LepR-positive NPY-hrGFP neurons (−0.7 ± 1.3 mV; resting membrane potential: −43.8 ± 0.9; n = 13; Fig. 3K). Similarly, in the presence of LY294002 (10 μM; 10 minutes), leptin failed to hyperpolarize all LepR-positive NPY-hrGFP neurons (−0.3 ± 1.6 mV; resting membrane potential: −44.1 ± 1.6 mV; n = 11; Fig. 3L). The requirement of PI3K signaling in the leptin-induced hyperpolarization of NPY/AgRP neurons was then assessed in AgRP neurons deficient for both p110α and p110β. The inactivation of both subunits did not lead to observable alterations in AgRP whole-cell conductance (commonly used as a measure of cell size) [32], nor were the

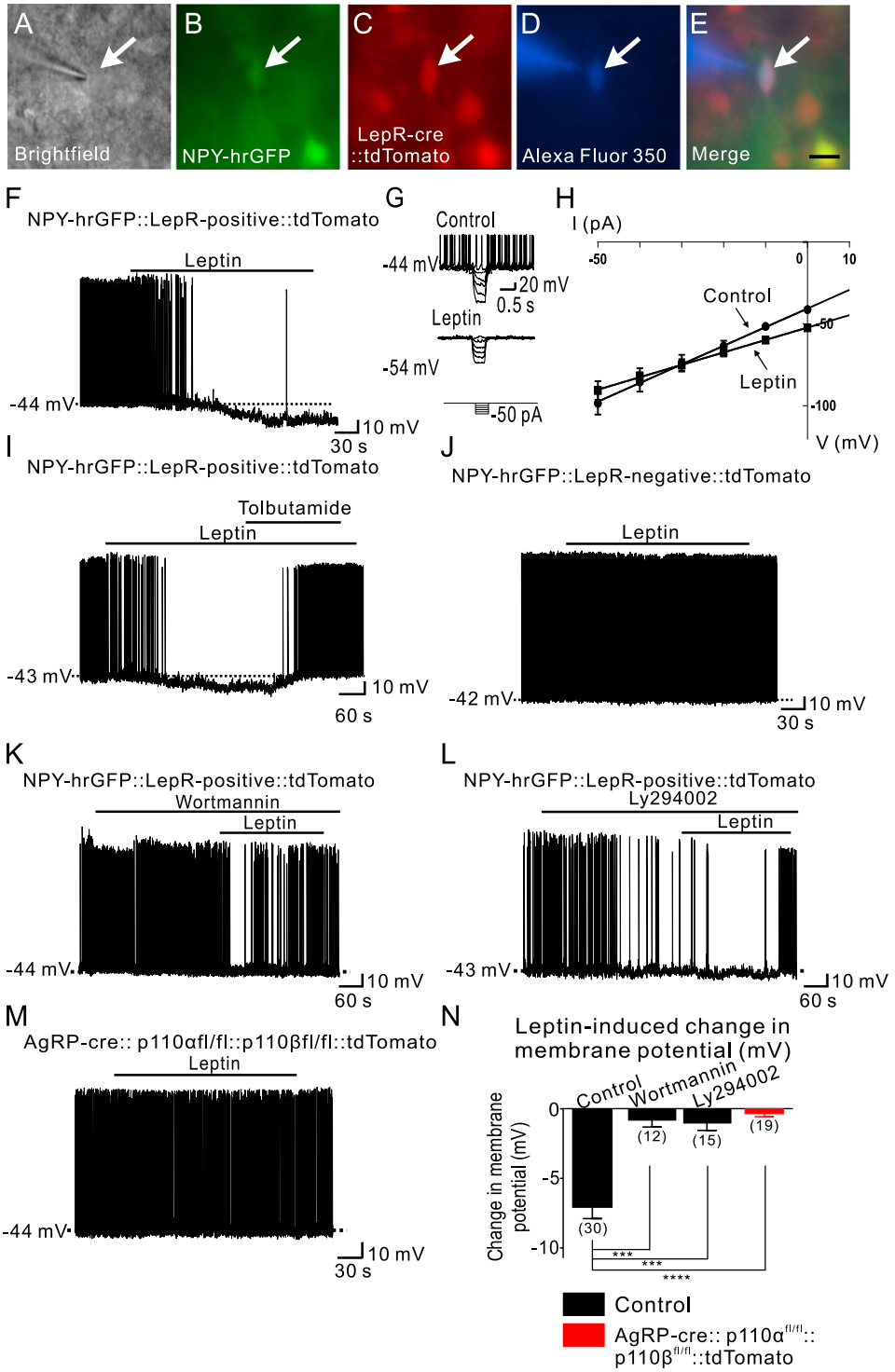

Figure 3. The leptin-induced hyperpolarization of LepR-positive NPY neurons requires both p110α and p110β catalytic subunits. (A) Bright-field illumination of NPY-hrGFP::LepR-cre::tdTomato neuron from NLT mice. (B) and (C) show the same neuron under fluorescein isothiocyanate (FITC; hrGFP) and Alexa Fluor 594 (tdTomato) illumination. Complete dialysis of Alexa Fluor 350 from the intracellular pipette is shown in (D) and (E) the merged image of targeted NPY neuron (arrow indicates the targeted cell). Scale bar, 50 μm. (F) Electrophysiological study demonstrates an NPY-hrGFP::Lepr-cre::tdTomato (green/red) neuron that was hyperpolarized in response to leptin. (G) Leptin administration decreases input resistance of NPY-hrGFP::Lepr-cre::tdTomato (green/red) neuron. (H) I-V relationship

of one NPY-hrGFP::Lepr-cre::tdTomato (green/red) neuron in response to leptin. (I) Administration of tolbutamide reverses the leptin-induced hyperpolarization of an NPY-hrGFP::Lepr-cre::tdTomato (green/red) neuron. (J) Leptin failed to affect the cellular activity of LepR-negative NPY (green) neurons. (K) Current-clamp recording demonstrates that pretreatment NPY-hrGFP::Lepr-cre::tdTomato (green/red) neurons with wortmannin diminished the leptin-induced hyperpolarization. (L) Pretreatment with LY294002 abolishes leptin-induced hyperpolarization of NPY-hrGFP::Lepr-cre::tdTomato (green/red) neurons. (M) Double deletion of p110α and p110β in AgRP neurons disrupts the leptin-induced hyperpolarization. (N) Histogram summarizes the leptin-induced change of membrane potential of NPY neurons from NLT mice with wortmannin and LY294002 treatment as well as AgRP neurons from APT mice. Error bars indicate SEM. ***$P < 0.001$; ****$P < 0.0001$.

resting membrane potential, basal firing rate, and whole-cell input resistance altered (Supplemental Fig. 5). Notably, in AgRP neurons with double deletion of p110α and p110β, leptin failed to induce a change in the membrane potential (-0.5 ± 0.4 mV; resting membrane potential: -41.3 ± 1.6 mV; n = 14; Fig. 3M). Taken together, these data suggest that both p110α and p110β subunits are required for the leptin-induced hyperpolarization of AgRP neurons (Fig. 3N).

D. Insulin Hyperpolarized NPY Neurons Rely on Both p110α and p110β

To assess the acute effects of insulin, both LepR-positive and -negative ARC NPY/AgRP neurons were targeted for electrophysiological recordings. Interestingly, ~94.4% of LepR-positive NPY-hrGFP neurons were hyperpolarized by insulin administration (50 nM; change in RMP: -17.4 ± 3.8 mV; resting membrane potential: -43.8 ± 1.4 mV; n = 17; Fig. 4A). Analogous to the results of leptin, we found that the insulin-induced hyperpolarization persisted after pretreatment of NPY-hrGFP neurons with 2 μM TTX followed by application of insulin (80%; change in RMP: -12.1 ± 3.1 mV; resting membrane potential: -43.7 ± 1.2 mV; n = 10; data not shown), supporting a direct membrane hyperpolarization of NPY neurons by insulin independent of action potential–mediated synaptic transmission. The insulin-induced hyperpolarization was accompanied by a decrease in the firing frequency and input resistance (33.3%; 1520 ± 80 MΩ for control, 1110 ± 110 MΩ for insulin; reversal membrane potential crossed at -90 ± 3.8 mV; n = 8; Fig. 4B and 4C). Notably, 94% of LepR-negative NPY-hrGFP neurons from the same mice were also hyperpolarized by insulin administration (change in RMP: -10.9 ± 2.4 mV; resting membrane potential: -41.3 ± 2.2 mV; n = 16; Fig. 4E). AgRP neurons deficient for InsRs (AgRP-cre::InsR-flox::tdTomato) failed to respond to insulin (change in RMP: -0.5 ± 0.3 mV; n = 15; Supplemental Fig. 4), supporting a requirement of InsRs in the acute change of cellular activity. The insulin-induced hyperpolarization of NPY-hrGFP neurons (both LepR-positive and -negative) was completely rescued after administration of tolbutamide (200 μM; n = 11; Fig. 4D), suggesting insulin can exert its acute inhibitory effects via activation of a K_{ATP} channel. To examine the requirement of PI3K signaling in the insulin-induced inhibition of NPY/AgRP, brain slices containing the ARC nucleus were pretreated with PI3K antagonists, wortmannin, and LY294002. The PI3K antagonists (100 nM wortmannin and 10 μM LY294002) abrogated the insulin-induced hyperpolarization of LepR-positive and -negative NPY-hrGFP neurons (wortmannin, change in RMP: -0.2 ± 1.3 mV; resting membrane potential: -44.4 ± 0.9 mV; n = 11, Fig. 4F; LY294002: change in RMP: -0.7 ± 1.6 mV; resting membrane potential: -45.1 ± 1.6 mV; n = 11; Fig. 4G). Interestingly, insulin also failed to hyperpolarize all AgRP neurons deficient for p110α and p110β (Fig. 4H). Collectively, these data suggest a mechanism in which both p110α and p110β subunits are necessary for the insulin-induced hyperpolarization of AgRP neurons (Fig. 4I).

E. AgRP-Specific Disruption of Both p110α and p110β Fails to Abrogate Activation of NPY/AgRP Neurons by Ghrelin

The acute effects of ghrelin were examined in NPY-hrGFP neurons that express and do not express LepRs. Notably, 7 out of 12 LepR-positive NPY-hrGFP neurons were depolarized by ghrelin administration, with a reversal membrane potential crossed at -25.8 ± 4.5 mV (58%;

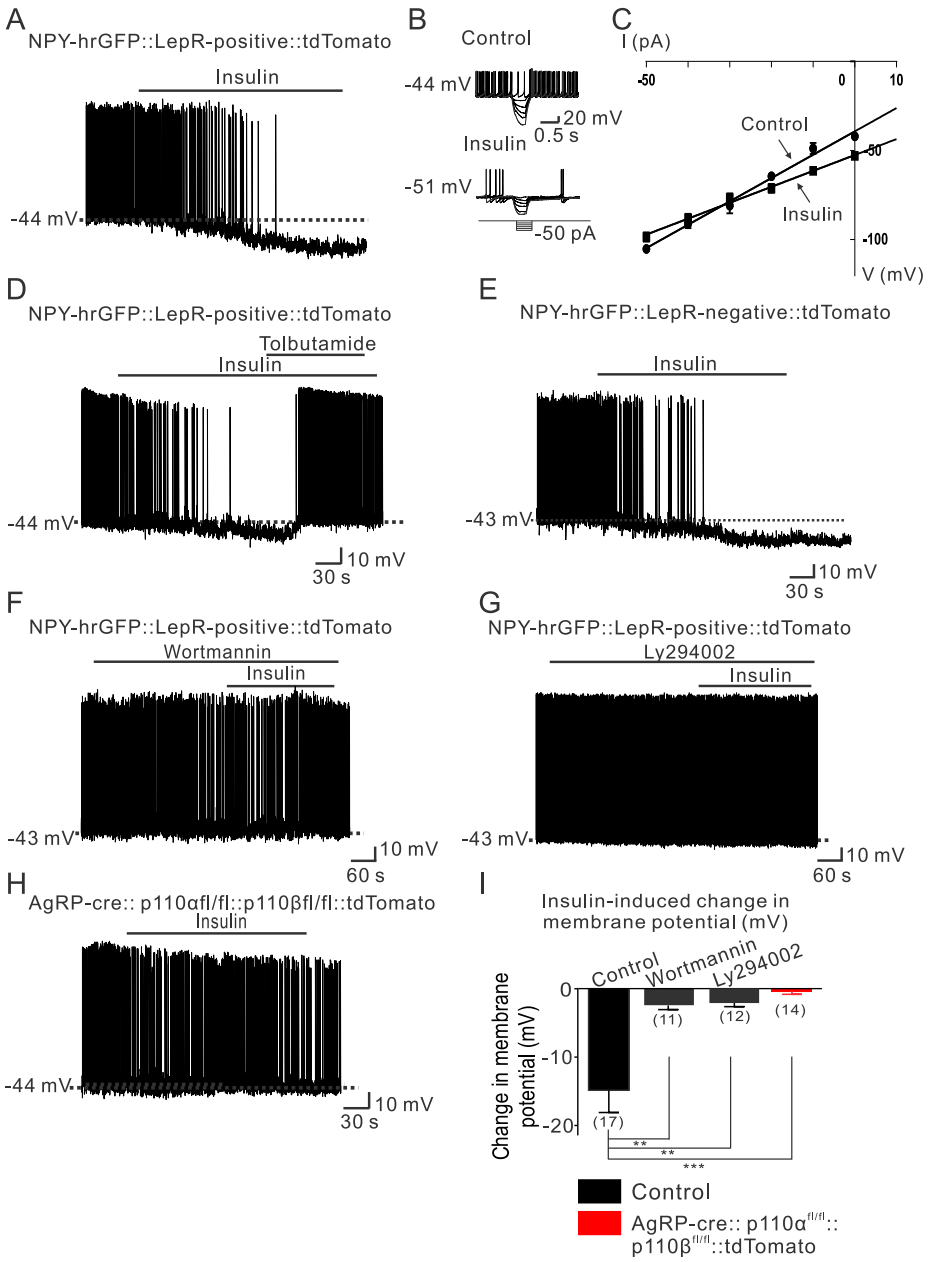

Figure 4. The insulin-induced hyperpolarization of NPY/AgRP neurons requires both p110α and p110β catalytic subunits. (A) Representative electrophysiological trace illustrates an NPY-hrGFP::Lepr-cre::tdTomato (green/red) neuron is hyperpolarized by insulin. (B) Insulin administration decreased input resistance of NPY-hrGFP::Lepr-cre::tdTomato (green/red) neurons. (C) I-V relationship of NPY-hrGFP::Lepr-cre::tdTomato (green/red) neurons in response to insulin. (D) Administration of tolbutamide rescues the hyperpolarization of NPY-hrGFP::Lepr-cre::tdTomato (green/red) neurons induced by insulin. (E) Current-clamp recording illustrating that insulin administration also hyperpolarized a LepR-negative NPY (green) neuron. (F) Representative electrophysiological trace shows that pretreatment NPY-hrGFP::Lepr-cre::tdTomato (green/red) neurons with (100 nM) wortmannin blocks insulin-induced hyperpolarization. (G) Insulin fails to hyperpolarize NPY-hrGFP::Lepr-cre:: tdTomato (green/red) neurons when pretreated with (10 μM) LY294002. (H) AgRP-specific deletion of both p110α and p110β abrogated the insulin-induced hyperpolarization. (I) Histogram illustrates the insulin-induced change of membrane potential of NPY neurons from NLT mice with wortmannin and LY294002 treatment as well as AgRP neurons from APT mice. Error bars indicate SEM. $^{**}P < 0.01$; $^{***}P < 0.001$.

5.3 ± 0.8 mV; resting membrane potential: −41.5 ± 1.1 mV; n = 7; Fig. 5A and 5C). A similar percentage of LepR-negative NPY-hrGFP neurons were activated in response to ghrelin (60%; change in RMP: 6.1 ± 1.1 mV; resting membrane potential: −41.1 ± 1.7 mV; n = 5; Fig. 5B). Pretreatment of NPY-hrGFP neurons with TTX and synaptic blockers failed to blunt the stimulatory effect of ghrelin (6.4 ± 1.2 mV; Fig. 5D), supporting a postsynaptic site of action. Additionally, a subset (n = 7) of LepR-positive NPY-hrGFP neurons were recorded in voltage clamp under normal recording conditions at a membrane potential of −70 mV, and application of ghrelin resulted in an inward current in four out of seven neurons (−23.4 ± 2.1 pA;

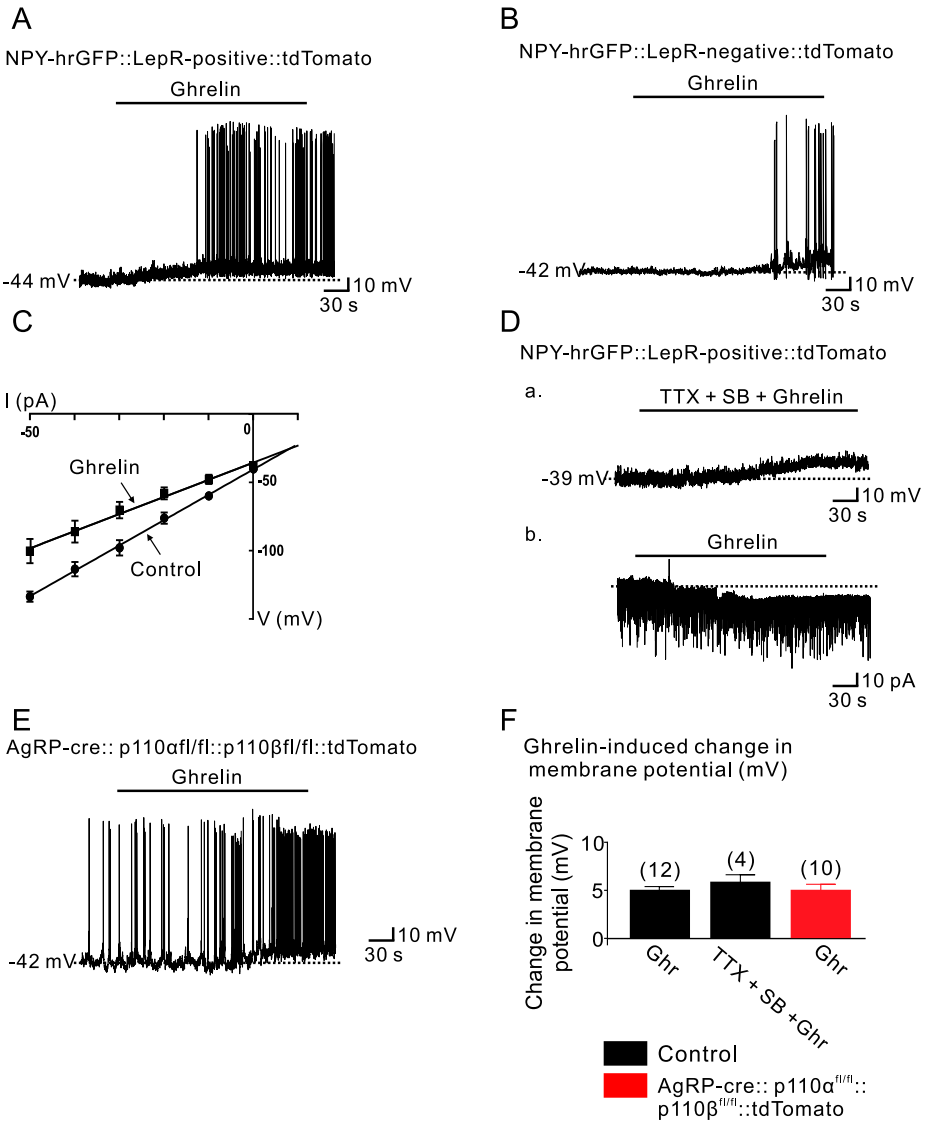

Figure 5. AgRP-specific disruption of both p110α and p110β fails to alter the ghrelin-induced activation of NPY/AgRP neurons. Electrophysiological trace demonstrating an (A) NPY-hrGFP::Lepr-cre::tdTomato (green/red) neuron and (B) NPY-hrGFP (green) neuron were depolarized by (100 nM) ghrelin. (C) I-V relationship of an NPY-hrGFP::Lepr-cre::tdTomato (green/red) neuron in response to ghrelin. (D) Pretreatment with (a) TTX (2 μM) and synaptic blockers (SB; CNQX, 10 μM; AP5, 50 μM; and picrotoxin, 50 μM) fails to abrogate the ghrelin-induced depolarization of NPY neurons, and (b) ghrelin application produced an inward current in the majority of NPY-hrGFP::Lepr-cre::tdTomato (green/red) neurons; holding potential is −70 mV. (E) Representative current-clamp record showing that AgRP-cre::p110$\alpha^{fl/fl}$::p110$\beta^{fl/fl}$ neurons are depolarized by (100 nM) ghrelin. (F) Histogram illustrates that AgRP-specific disruption of both p110α and p110β fails to alter the ghrelin-induced depolarization. Error bars indicate SEM.

n = 4; Fig. 5D). Previous reports suggest ghrelin stimulates NPY/AgRP neurons independent of PI3K signaling [33, 34]. Accordingly, AgRP neurons deficient for both p110α and p110β were responsive to the excitatory effects of ghrelin (Fig. 5E). Together, these data suggest that ghrelin activates NPY/AgRP neurons irrespective of LepR expression via activation of a mixed cation channel. Moreover, deletion of both p110α and p110β fails to abrogate this effect, implying that p110α and p110β deficiency in AgRP neurons results in a selective loss of PI3K-dependent changes of cellular activity, which include leptin and insulin.

3. Discussion

Selective deficiency of the PI3K catalytic subunits p110α and p110β in murine AgRP neurons resulted in increased body weight concomitant with decreased energy expenditure independent of changes in food intake. Loss of p110α and p110β in AgRP neurons also impaired glucose and insulin sensitivity. The cellular mechanism of leptin and insulin to elicit acute electrophysiological responses requires both p110α and p110β in NPY/AgRP neurons. Together, these data support a model in which loss of PI3K signaling in NPY/AgRP neurons abrogates the acute inhibitory actions of leptin and insulin in NPY/AgRP neurons, culminating in a positive energy balance and dysregulation of glucose metabolism.

The PI3K signaling pathway is involved in a variety of physiological processes including metabolic regulation. Pharmacological inhibition or global genetic deficiency of PI3K lowers body weight and fat mass by increasing white adipose tissue lipolysis and browning [35, 36]. Numerous physiological effects of leptin and insulin action via PI3K to regulate energy balance are suggested to involve the central nervous system [8, 31, 37, 38]. In particular, overactivation of PI3K signaling in LepR-positive cells resulted in a lean phenotype coincident with browning of white adipose tissue [32]. Similarly, loss of p110α and p110β in LepR-positive cells resulted in a lean phenotype associated with increased energy expenditure and thermogenesis [39]. Although these studies suggest regulation of PTEN by PI3K catalytic subunits with overlapping effects in metabolism, the role of NPY/AgRP neurons in this activity remains undefined. In the ARC, the catalytic PI3K subunits p110α and p110β, but not p110δ, are highly expressed [14]. Surprisingly, genetic inactivation of the p110β subunit in AgRP neurons resulted in a resistance to diet-induced obesity, whereas AgRP p110α-null mice failed to alter energy regulation [8]. It is important to note that studies using PI3K inhibitors, such as wortmannin or LY294002, fail to distinguish effects of specific PI3K subunits (both regulatory and catalytic). Although the use of subunit-specific conditional alleles allows for detailed investigation of PI3K signaling and functions, this strategy does not account for the complementary action and compensatory mechanism within p110α and p110β in the hypothalamus [40, 41]. To better examine the requirement of PI3K signaling in AgRP neurons to regulate energy balance and glucose homeostasis, we inactivated both p110α and p110β in AgRP neurons. AgRP neuron–specific p110α and p110β deletion decreased energy expenditure independent of changing food intake, ultimately leading to increased adiposity and lean mass. NPY/AgRP neurons and their congnate activity have been studied extensively in regulating feeding behavior [1, 3, 4, 42–44]. However, the current study demonstrates that loss of PI3K catalytic subunits abrogates the acute effects of leptin and insulin on the cellular activity of NPY neurons while at the same time failing to influence feeding. The lack of effect on food intake in the current study may be less surprising given that loss of LepRs in AgRP neurons increases body weight independent of altered feeding [45]. Similar effects were observed in mice deficient for LepRs in pro-opiomelanocortin (POMC) neurons [23]. Interestingly, loss of LepRs in both POMC and AgRP neurons produces hyperphagia, suggesting an important interaction between POMC and AgRP neurons in the regulation of feeding behavior by leptin. It is currently unclear if p110α and p110β is required in the leptin-dependent regulation of feeding by both POMC and AgRP neurons. However, the current study supports a p110α- and p110β-dependent regulation of energy balance in AgRP neurons independent of altered food intake.

In addition to energy homeostasis, PI3K inhibitors have been shown to elevate blood glucose levels potentially by perturbing insulin signaling [46–49]. In the central nervous system, intracerebroventricular insulin treatment activated hypothalamic InsR substrate–PI3K signaling [38]. The reduction of hepatic glucose production was induced by intracerebroventricular administration of insulin, which could be blocked by PI3K inhibitors [38, 49]. In the current study, deficiency of both PI3K catalytic subunits (p110α and p110β) in AgRP neurons impaired glucose and insulin sensitivity in mice. We speculate PI3K signaling in AgRP neurons might be a cellular link in the insulin-induced regulatory effect on glucose.

The acute activity of AgRP neurons has been closely linked to the regulation of energy balance and glucose homeostasis [1, 3, 4, 43, 50]. In particular, acute activation of AgRP neurons induced insulin resistance by inhibiting glucose uptake of brown adipose tissue [4]. Interestingly, the metabolic effectors leptin and insulin suppress the activity of AgRP neurons [6, 8, 9, 31, 51]. In the current study, the inhibitory effect of leptin required both LepRs and K_{ATP} channels. Additionally, inactivation of PI3K signaling via concurrent deficiency of p110α and p110β blunted the leptin-induced hyperpolarization in AgRP neurons. Similar to leptin, insulin also inhibited the activity of AgRP neurons via an InsR-dependent activation of PI3K catalytic subunits (p110α and p110β) and a downstream K_{ATP} channel. However, it is important to note that electrophysiological assessments of the circulating factors: leptin and insulin on NPY/AgRP neurons has been somewhat controversial. In agreement with several previous reports, in the current study, both leptin and insulin inhibit NPY/AgRP neurons [6–9, 31, 51, 52]. Notably, we failed to detect activation of any NPY/AgRP neurons recorded in response to either leptin or insulin; however, a few studies show no effect or a stimulatory activity of these compounds on NPY/AgRP neurons [8, 53]. Additionally, a recent report failed to detect changes in NPY/AgRP-specific calcium dynamics *in vivo* in response to several peripherally administered compounds, including leptin [54]. A possible explanation for these conflicting results might be due to the fact that approximately one-half of NPY-hrGFP neurons in ARC nucleus express LepRs. Moreover, recent evidence suggests hypothalamic neurons are markedly heterogeneous [29, 55–58]. Thus, the authors cannot eliminate the possibility that leptin- and insulin-induced changes in neuronal activity might be obfuscated due to cellular heterogeneity and inherent limitations of targeting responsive cells. An attempt to eliminate such selection biases was made by targeting NPY/AgRP neurons throughout the rostral-caudal axis. Moreover, the acute electrophysiological responses of leptin and insulin were absent in mice deficient for LepR and InsR in AgRP neurons, suggesting that the changes in cellular activity were specific to cognate receptors for leptin and insulin, respectively. Ultimately, these data suggest that endogenously expressed circulating factors, which alter the activity of NPY/AgRP neurons, may have profound effects on metabolism. Moreover, the heterogeneity and distribution of LepRs and InsRs might be important facets in determining the physiological effects of these factors.

4. Conclusion

In summary, the current study demonstrates that deficiency of PI3K subunits (p110α and p110β) in ARC NPY/AgRP neurons impaired energy balance and glucose homeostasis. PI3K catalytic subunits were also required in NPY/AgRP neurons for the acute effects of insulin and leptin on cellular activity. Together, these data provide evidence for PI3K as a substrate for both leptin and insulin to regulate energy balance and glucose metabolism in NPY/AgRP neurons.

Acknowledgments

We thank Dr. Joel K. Elmquist (Division of Hypothalamic Research, Department of Internal Medicine, The University of Texas Southwestern Medical Center, Dallas, TX) for providing the NPY-hrGFP and AgRP-cre mice and The Guangdong Provincial Clinical Medical Centre for Neurosurgery for help.

Financial Support: This work was supported by Grant R01-DK-100699 from the National Institute of Diabetes and Digestive and Kidney Diseases to K.W.W. and by Grant 2013B020400005 from The Guangdong Provincial Clinical Medical Centre for Neurosurgery.

Correspondence: Hongbo Guo, MD, The National Key Clinical Specialty, The Engineering Technology Research Center of Education Ministry of China, Guangdong Provincial Key Laboratory on Brain Function Repair and Regeneration, Department of Neurosurgery, 253 GongYe Road, Zhujiang Hospital, Southern Medical University, Guangzhou 510282, China. E-mail: guohongbo911@126.com; or Kevin W. Williams, PhD, The University of Texas Southwestern Medical Center, 5323 Harry Hines Boulevard, Dallas, Texas 75390. E-mail: kevin.williams@utsouthwestern.edu.

Disclosure Summary: The authors have nothing to disclose.

References and Notes

1. Aponte Y, Atasoy D, Sternson SM. AGRP neurons are sufficient to orchestrate feeding behavior rapidly and without training. *Nat Neurosci*. 2011;**14**(3):351–355.
2. Burke LK, Darwish T, Cavanaugh AR, Virtue S, Roth E, Morro J, Liu SM, Xia J, Dalley JW, Burling K, Chua S, Vidal-Puig T, Schwartz GJ, Blouet C. mTORC1 in AGRP neurons integrates exteroceptive and interoceptive food-related cues in the modulation of adaptive energy expenditure in mice. *eLife*. 2017;**6**:6.
3. Krashes MJ, Koda S, Ye C, Rogan SC, Adams AC, Cusher DS, Maratos-Flier E, Roth BL, Lowell BB. Rapid, reversible activation of AgRP neurons drives feeding behavior in mice. *J Clin Invest*. 2011; **121**(4):1424–1428.
4. Steculorum SM, Ruud J, Karakasilioti I, Backes H, Engström Ruud L, Timper K, Hess ME, Tsaousidou E, Mauer J, Vogt MC, Paeger L, Bremser S, Klein AC, Morgan DA, Frommolt P, Brinkkötter PT, Hammerschmidt P, Benzing T, Rahmouni K, Wunderlich FT, Kloppenburg P, Brüning JC. AgRP neurons control systemic insulin sensitivity via myostatin expression in brown adipose tissue. *Cell*. 2016;**165**(1):125–138.
5. Garfield AS, Shah BP, Burgess CR, Li MM, Li C, Steger JS, Madara JC, Campbell JN, Kroeger D, Scammell TE, Tannous BA, Myers MG Jr, Andermann ML, Krashes MJ, Lowell BB. Dynamic GABAergic afferent modulation of AgRP neurons. *Nat Neurosci*. 2016;**19**(12):1628–1635.
6. Spanswick D, Smith MA, Mirshamsi S, Routh VH, Ashford ML. Insulin activates ATP-sensitive K+ channels in hypothalamic neurons of lean, but not obese rats. *Nat Neurosci*. 2000;**3**(8):757–758.
7. Baver SB, Hope K, Guyot S, Bjørbaek C, Kaczorowski C, O'Connell KM. Leptin modulates the intrinsic excitability of AgRP/NPY neurons in the arcuate nucleus of the hypothalamus. *J Neurosci*. 2014;**34**(16): 5486–5496.
8. Al-Qassab H, Smith MA, Irvine EE, Guillermet-Guibert J, Claret M, Choudhury AI, Selman C, Piipari K, Clements M, Lingard S, Chandarana K, Bell JD, Barsh GS, Smith AJ, Batterham RL, Ashford ML, Vanhaesebroeck B, Withers DJ. Dominant role of the p110beta isoform of PI3K over p110alpha in energy homeostasis regulation by POMC and AgRP neurons. *Cell Metab*. 2009;**10**(5):343–354.
9. Könner AC, Janoschek R, Plum L, Jordan SD, Rother E, Ma X, Xu C, Enriori P, Hampel B, Barsh GS, Kahn CR, Cowley MA, Ashcroft FM, Brüning JC. Insulin action in AgRP-expressing neurons is required for suppression of hepatic glucose production. *Cell Metab*. 2007;**5**(6):438–449.
10. Varela L, Horvath TL. Leptin and insulin pathways in POMC and AgRP neurons that modulate energy balance and glucose homeostasis. *EMBO Rep*. 2012;**13**(12):1079–1086.
11. Mirshamsi S, Laidlaw HA, Ning K, Anderson E, Burgess LA, Gray A, Sutherland C, Ashford ML. Leptin and insulin stimulation of signalling pathways in arcuate nucleus neurones: PI3K dependent actin reorganization and KATP channel activation. *BMC Neurosci*. 2004;**5**(1):54.
12. Morrison CD, Morton GJ, Niswender KD, Gelling RW, Schwartz MW. Leptin inhibits hypothalamic Npy and Agrp gene expression via a mechanism that requires phosphatidylinositol 3-OH-kinase signaling. *Am J Physiol Endocrinol Metab*. 2005;**289**(6):E1051–E1057.
13. Xu AW, Kaelin CB, Takeda K, Akira S, Schwartz MW, Barsh GS. PI3K integrates the action of insulin and leptin on hypothalamic neurons. *J Clin Invest*. 2005;**115**(4):951–958.
14. Vanhaesebroeck B, Ali K, Bilancio A, Geering B, Foukas LC. Signalling by PI3K isoforms: insights from gene-targeted mice. *Trends Biochem Sci*. 2005;**30**(4):194–204.
15. Brachmann SM, Yballe CM, Innocenti M, Deane JA, Fruman DA, Thomas SM, Cantley LC. Role of phosphoinositide 3-kinase regulatory isoforms in development and actin rearrangement. *Mol Cell Biol*. 2005;**25**(7):2593–2606.
16. Chaussade C, Rewcastle GW, Kendall JD, Denny WA, Cho K, Grønning LM, Chong ML, Anagnostou SH, Jackson SP, Daniele N, Shepherd PR. Evidence for functional redundancy of class IA PI3K isoforms in insulin signalling. *Biochem J*. 2007;**404**(3):449–458.
17. Sun J, Gao Y, Yao T, Huang Y, He Z, Kong X, Yu K-J, Wang R-T, Guo H, Yan J, Chang Y, Chen H, Scherer PE, Liu T, Williams KW. Adiponectin potentiates the acute effects of leptin in arcuate Pomc neurons. *Mol Metab*. 2016;**5**(10):882–891.

18. Scott MM, Lachey JL, Sternson SM, Lee CE, Elias CF, Friedman JM, Elmquist JK. Leptin targets in the mouse brain. *J Comp Neurol*. 2009;**514**(5):518–532.
19. van den Pol AN, Yao Y, Fu LY, Foo K, Huang H, Coppari R, Lowell BB, Broberger C. Neuromedin B and gastrin-releasing peptide excite arcuate nucleus neuropeptide Y neurons in a novel transgenic mouse expressing strong Renilla green fluorescent protein in NPY neurons. *J Neurosci*. 2009;**29**(14):4622–4639.
20. Zhao JJ, Cheng H, Jia S, Wang L, Gjoerup OV, Mikami A, Roberts TM. The p110alpha isoform of PI3K is essential for proper growth factor signaling and oncogenic transformation. *Proc Natl Acad Sci USA*. 2006;**103**(44):16296–16300.
21. Jia S, Liu Z, Zhang S, Liu P, Zhang L, Lee SH, Zhang J, Signoretti S, Loda M, Roberts TM, Zhao JJ. Essential roles of PI(3)K-p110beta in cell growth, metabolism and tumorigenesis [published correction appears in Nature. 2016;**533**(7602):278]. *Nature*. 2008;**454**(7205):776–779.
22. Tong Q, Ye CP, Jones JE, Elmquist JK, Lowell BB. Synaptic release of GABA by AgRP neurons is required for normal regulation of energy balance. *Nat Neurosci*. 2008;**11**(9):998–1000.
23. Balthasar N, Coppari R, McMinn J, Liu SM, Lee CE, Tang V, Kenny CD, McGovern RA, Chua SC Jr, Elmquist JK, Lowell BB. Leptin receptor signaling in POMC neurons is required for normal body weight homeostasis. *Neuron*. 2004;**42**(6):983–991.
24. Brüning JC, Gautam D, Burks DJ, Gillette J, Schubert M, Orban PC, Klein R, Krone W, Müller-Wieland D, Kahn CR. Role of brain insulin receptor in control of body weight and reproduction. *Science*. 2000;**289**(5487):2122–2125.
25. Hill JW, Williams KW, Ye C, Luo J, Balthasar N, Coppari R, Cowley MA, Cantley LC, Lowell BB, Elmquist JK. Acute effects of leptin require PI3K signaling in hypothalamic proopiomelanocortin neurons in mice. *J Clin Invest*. 2008;**118**(5):1796–1805.
26. Williams KW, Liu T, Kong X, Fukuda M, Deng Y, Berglund ED, Deng Z, Gao Y, Liu T, Sohn JW, Jia L, Fujikawa T, Kohno D, Scott MM, Lee S, Lee CE, Sun K, Chang Y, Scherer PE, Elmquist JK. Xbp1s in Pomc neurons connects ER stress with energy balance and glucose homeostasis. *Cell Metab*. 2014;**20**(3):471–482.
27. Elias CF, Aschkenasi C, Lee C, Kelly J, Ahima RS, Bjorbaek C, Flier JS, Saper CB, Elmquist JK. Leptin differentially regulates NPY and POMC neurons projecting to the lateral hypothalamic area. *Neuron*. 1999;**23**(4):775–786.
28. Elias CF, Kelly JF, Lee CE, Ahima RS, Drucker DJ, Saper CB, Elmquist JK. Chemical characterization of leptin-activated neurons in the rat brain. *J Comp Neurol*. 2000;**423**(2):261–281.
29. Williams KW, Margatho LO, Lee CE, Choi M, Lee S, Scott MM, Elias CF, Elmquist JK. Segregation of acute leptin and insulin effects in distinct populations of arcuate proopiomelanocortin neurons. *J Neurosci*. 2010;**30**(7):2472–2479.
30. Franklin KBJ, Paxinos G. *The Mouse Brain in Stereotaxic Coordinates*. 3rd ed. Amsterdam: Elsevier; 2007.
31. van den Top M, Lee K, Whyment AD, Blanks AM, Spanswick D. Orexigen-sensitive NPY/AgRP pacemaker neurons in the hypothalamic arcuate nucleus. *Nat Neurosci*. 2004;**7**(5):493–494.
32. Plum L, Rother E, Münzberg H, Wunderlich FT, Morgan DA, Hampel B, Shanabrough M, Janoschek R, Könner AC, Alber J, Suzuki A, Krone W, Horvath TL, Rahmouni K, Brüning JC. Enhanced leptin-stimulated Pi3k activation in the CNS promotes white adipose tissue transdifferentiation. *Cell Metab*. 2007;**6**(6):431–445.
33. Cowley MA, Smith RG, Diano S, Tschöp M, Pronchuk N, Grove KL, Strasburger CJ, Bidlingmaier M, Esterman M, Heiman ML, Garcia-Segura LM, Nillni EA, Mendez P, Low MJ, Sotonyi P, Friedman JM, Liu H, Pinto S, Colmers WF, Cone RD, Horvath TL. The distribution and mechanism of action of ghrelin in the CNS demonstrates a novel hypothalamic circuit regulating energy homeostasis. *Neuron*. 2003; **37**(4):649–661.
34. Kohno D, Nakata M, Maekawa F, Fujiwara K, Maejima Y, Kuramochi M, Shimazaki T, Okano H, Onaka T, Yada T. Leptin suppresses ghrelin-induced activation of neuropeptide Y neurons in the arcuate nucleus via phosphatidylinositol 3-kinase- and phosphodiesterase 3-mediated pathway. *Endocrinology*. 2007;**148**(5):2251–2263.
35. Ortega-Molina A, Lopez-Guadamillas E, Mattison JA, Mitchell SJ, Muñoz-Martin M, Iglesias G, Gutierrez VM, Vaughan KL, Szarowicz MD, González-García I, López M, Cebrián D, Martinez S, Pastor J, de Cabo R, Serrano M. Pharmacological inhibition of PI3K reduces adiposity and metabolic syndrome in obese mice and rhesus monkeys. *Cell Metab*. 2015;**21**(4):558–570.
36. Perino A, Beretta M, Kilić A, Ghigo A, Carnevale D, Repetto IE, Braccini L, Longo D, Liebig-Gonglach M, Zaglia T, Iacobucci R, Mongillo M, Wetzker R, Bauer M, Aime S, Vercelli A, Lembo G, Pfeifer A, Hirsch E. Combined inhibition of PI3Kβ and PI3Kγ reduces fat mass by enhancing α-MSH-dependent sympathetic drive. *Sci Signal*. 2014;**7**(352):ra110.

37. Niswender KD, Morton GJ, Stearns WH, Rhodes CJ, Myers MG Jr, Schwartz MW. Intracellular signalling. Key enzyme in leptin-induced anorexia. *Nature*. 2001;**413**(6858):794–795.
38. Niswender KD, Morrison CD, Clegg DJ, Olson R, Baskin DG, Myers MG Jr, Seeley RJ, Schwartz MW. Insulin activation of phosphatidylinositol 3-kinase in the hypothalamic arcuate nucleus: a key mediator of insulin-induced anorexia. *Diabetes*. 2003;**52**(2):227–231.
39. Garcia-Galiano D, Borges BC, Donato J Jr, Allen SJ, Bellefontaine N, Wang M, Zhao JJ, Kozloff KM, Hill JW, Elias CF. PI3Kα inactivation in leptin receptor cells increases leptin sensitivity but disrupts growth and reproduction. *JCI Insight*. 2017;**2**(23):2.
40. Graupera M, Guillermet-Guibert J, Foukas LC, Phng LK, Cain RJ, Salpekar A, Pearce W, Meek S, Millan J, Cutillas PR, Smith AJ, Ridley AJ, Ruhrberg C, Gerhardt H, Vanhaesebroeck B. Angiogenesis selectively requires the p110alpha isoform of PI3K to control endothelial cell migration. *Nature*. 2008; **453**(7195):662–666.
41. Guillermet-Guibert J, Bjorklof K, Salpekar A, Gonella C, Ramadani F, Bilancio A, Meek S, Smith AJ, Okkenhaug K, Vanhaesebroeck B. The p110beta isoform of phosphoinositide 3-kinase signals downstream of G protein-coupled receptors and is functionally redundant with p110gamma. *Proc Natl Acad Sci USA*. 2008;**105**(24):8292–8297.
42. Atasoy D, Aponte Y, Su HH, Sternson SM. A FLEX switch targets Channelrhodopsin-2 to multiple cell types for imaging and long-range circuit mapping. *J Neurosci*. 2008;**28**(28):7025–7030.
43. Betley JN, Cao ZF, Ritola KD, Sternson SM. Parallel, redundant circuit organization for homeostatic control of feeding behavior. *Cell*. 2013;**155**(6):1337–1350.
44. Dietrich MO, Zimmer MR, Bober J, Horvath TL. Hypothalamic Agrp neurons drive stereotypic behaviors beyond feeding [published correction appears in *Cell*. 2017;**169**(3):559]. *Cell*. 2015;**160**(6):1222–1232.
45. van de Wall E, Leshan R, Xu AW, Balthasar N, Coppari R, Liu SM, Jo YH, MacKenzie RG, Allison DB, Dun NJ, Elmquist J, Lowell BB, Barsh GS, de Luca C, Myers MG Jr, Schwartz GJ, Chua SC Jr. Collective and individual functions of leptin receptor modulated neurons controlling metabolism and ingestion. *Endocrinology*. 2008;**149**(4):1773–1785.
46. Fruman DA, Chiu H, Hopkins BD, Bagrodia S, Cantley LC, Abraham RT. The PI3K pathway in human disease. *Cell*. 2017;**170**(4):605–635.
47. Huang S, Czech MP. The GLUT4 glucose transporter. *Cell Metab*. 2007;**5**(4):237–252.
48. Katome T, Obata T, Matsushima R, Masuyama N, Cantley LC, Gotoh Y, Kishi K, Shiota H, Ebina Y. Use of RNA interference-mediated gene silencing and adenoviral overexpression to elucidate the roles of AKT/protein kinase B isoforms in insulin actions. *J Biol Chem*. 2003;**278**(30):28312–28323.
49. Gelling RW, Morton GJ, Morrison CD, Niswender KD, Myers MG Jr, Rhodes CJ, Schwartz MW. Insulin action in the brain contributes to glucose lowering during insulin treatment of diabetes. *Cell Metab*. 2006;**3**(1):67–73.
50. Atasoy D, Betley JN, Su HH, Sternson SM. Deconstruction of a neural circuit for hunger. *Nature*. 2012; **488**(7410):172–177.
51. Spanswick D, Smith MA, Groppi VE, Logan SD, Ashford ML. Leptin inhibits hypothalamic neurons by activation of ATP-sensitive potassium channels. *Nature*. 1997;**390**(6659):521–525.
52. Qiu J, Zhang C, Borgquist A, Nestor CC, Smith AW, Bosch MA, Ku S, Wagner EJ, Rønnekleiv OK, Kelly MJ. Insulin excites anorexigenic proopiomelanocortin neurons via activation of canonical transient receptor potential channels. *Cell Metab*. 2014;**19**(4):682–693.
53. Claret M, Smith MA, Batterham RL, Selman C, Choudhury AI, Fryer LG, Clements M, Al-Qassab H, Heffron H, Xu AW, Speakman JR, Barsh GS, Viollet B, Vaulont S, Ashford ML, Carling D, Withers DJ. AMPK is essential for energy homeostasis regulation and glucose sensing by POMC and AgRP neurons. *J Clin Invest*. 2007;**117**(8):2325–2336.
54. Beutler LR, Chen Y, Ahn JS, Lin YC, Essner RA, Knight ZA. Dynamics of gut-brain communication underlying hunger. *Neuron*. 2017;**96**(2):461–475.
55. Henry FE, Sugino K, Tozer A, Branco T, Sternson SM. Cell type-specific transcriptomics of hypothalamic energy-sensing neuron responses to weight-loss. *eLife*. 2015;**4**:4.
56. Lam BYH, Cimino I, Polex-Wolf J, Nicole Kohnke S, Rimmington D, Iyemere V, Heeley N, Cossetti C, Schulte R, Saraiva LR, Logan DW, Blouet C, O'Rahilly S, Coll AP, Yeo GSH. Heterogeneity of hypothalamic pro-opiomelanocortin-expressing neurons revealed by single-cell RNA sequencing. *Mol Metab*. 2017;**6**(5):383–392.
57. Campbell JN, Macosko EZ, Fenselau H, Pers TH, Lyubetskaya A, Tenen D, Goldman M, Verstegen AM, Resch JM, McCarroll SA, Rosen ED, Lowell BB, Tsai LT. A molecular census of arcuate hypothalamus and median eminence cell types. *Nat Neurosci*. 2017;**20**(3):484–496.
58. Chen R, Wu X, Jiang L, Zhang Y. Single-cell RNA-Seq reveals hypothalamic cell diversity. *Cell Reports*. 2017;**18**(13):3227–3241.